

Digital Image Processing

The IBM Image Processing Facility is described and the mosaicking of LANDSAT imagery and multispectral classification of mineral deposits are discussed.

IBM IMAGE PROCESSING FACILITY

AN INTERACTIVE Image Processing Facility (IPF) has been developed to process earth-observation image data. The capability of the system allows a user to perform geometric and radiometric correction of image data, enhance the data, determine image characteristics and statistics, perform information extraction operations, and view the image products. The objectives of

analog, or standard photographic processes or by combinations of these techniques. Figure 1 shows the system configuration of the IPF. Off-line equipment digitizes and records image data. The processing of the data is performed on-line in an operator interactive manner by the use of displays and terminals. Table 1 summarizes the performance characteristics of the IPF peripheral devices. Most forms of human readable image data can be digitized, displayed, and recorded.

ABSTRACT: The use of digital sensors in earth resources applications appears to be well-established. The signals sent to the ground from the LANDSAT (previously known as the Earth Resources Technology Satellite, ERTS) Multispectral Scanner (MSS) are digitized prior to transmission.^{1,2} For future earth-observation programs, both the sensor outputs and the ground processing will be digital.³ If such sensors are to serve a useful role in the surveying and management of the earth's resources, efficient methods for correcting and extracting information from the sensor outputs must be developed. The Federal Systems Division of IBM has developed an image processing facility to experimentally process, view, and record digital image data. This facility has been used to support LANDSAT digital image processing investigations and advanced image processing research and development. A brief description of the facility is presented, some techniques that have been developed to correct the image data are discussed, and some results obtained by users of the facility are described.

the facility are to provide an investigator with the means to process data in a research and development manner in order to develop and evaluate advanced techniques and programs.

SYSTEM DESCRIPTION

Imagery can be provided to the IPF on computer compatible tape (CCT), high-resolution photographic film, or hard-copy form (maps, charts, or line graphic prints). The processing may be performed by digital,

IPF SOFTWARE

The IPF operates under the Time Sharing Option (TSO) of the IBM Operating System. The IPF software structure is shown in Figure 2. The IPF Interactive Programming System provides a user with a set of analysis tools for digital image manipulation and processing. It employs a user-oriented language which includes a set of commands and associated operands that selects the image to be processed, implements the processing func-

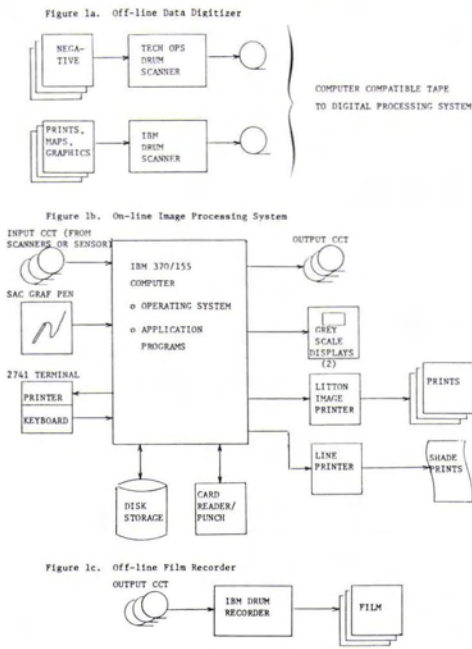


FIG. 1. IBM Image Processing Facility.

tions to be invoked, and outputs the processed image. Table 2 summarizes the applications programs that can be selected by the operator.

IMAGE PROCESSING TECHNIQUES

A significant amount of effort has been expended in the development of digital techniques for radiometric correction, geometric correction, and mosaicking of LANDSAT MSS scenes.⁴⁻⁷ Each of these areas is discussed in the following sections.

RADIOMETRIC CORRECTION

This section discusses both the nominal radiometric calibration/correction of the MSS data and the supplemental calibration which can be applied if the nominal methods fail fully to compensate for differences in the detectors.

Nominal Calibration/Correction. The nominal method for calibrating the outputs of

the 24 MSS detectors is adequately described elsewhere in the literature.² Basically, an on-board incandescent lamp and a variable neutral density filter are used to establish points on the input/output curve of each detector. Occasional solar observations are used to correct for changes in the output of the lamp. In this way, gradual changes in the output of each detector can be detected and measured.

The MSS detector outputs are digitized prior to transmission to the ground. Since six-bit quantization is used, each detector can produce only 64 discrete values. The calibration data can be used to construct for each detector a table which specifies the "correct" radiometric intensity for each value output by the detector. Radiometric correction can thus be reduced to a simple table look-up operation in which a value output by a given detector is used to extract the "correct" value from the correction table. Although a unique table is required for each of the 24 detectors, the storage to accommodate these tables is quite small by present computer standards.

Supplemental Calibration. These nominal techniques do not always fully compensate for differences in the outputs of the various MSS detectors. When this occurs, the effects are sometimes sufficiently large to produce visible horizontal "stripes" or "banding" in the images. Supplemental calibration can often be used to reduce these effects below the level of visual detectability.

There are several possible approaches to supplemental calibration. One is to note the response of each detector in areas of uniform radiance at different intensity levels. Another approach is to compile histograms of the responses of the detectors over a large number of data samples. In all cases, the object is to measure the differences in the "corrected" response curves of the detectors in each spectral band. These measurements then can be used to modify the nominal radiometric correction tables to produce identical corrected response curves for the detectors in each band.

It should be emphasized that supplemental calibration provides only a cosmetic correction. Unlike the nominal calibration techniques, supplemental calibration does not attempt to make the detector outputs correct. It only attempts to make them equal.

GEOMETRIC CORRECTION

This section discusses the geometric errors present in the MSS data, methods of measuring those errors, formation and application of a geometric correction function, and resam-



FIG. 2. IPF software structure.

TABLE 1. CHARACTERISTICS OF IPF PERIPHERALS AND TERMINALS.

| | IBM Drum Scanner | Tech-ops Film Scanner | IBM Film Plotter | Litton Imagery Printer | PEP GSGT Grey Scale Display | PEP 801 Grey Scale Display |
|--|--------------------------------|------------------------|-----------------------------------|------------------------|-----------------------------|-----------------------------|
| Input Form | Opaque documents, prints, maps | Photo film | 9 track tape (800/1600 bpi) | On-line to computer | On-line to computer | On-line to computer |
| Output Form | 9 track tape (800/1600 bpi) | 9 track tape (800 bpi) | Photo film (Negative or positive) | Photo print | CRT display | CRT display |
| Largest I/O document or display (mm) | 610 by 762 | 200 by 250 | 610 by 762 | 216 by 211 | 254 by 254 | 254 by 254 |
| Largest Raster | 30,000/24,000 | 9598/7998 | 30,000/24,000 | 1536/1536 | 1024/1024 | 1024/1024 |
| Resolution (spot size, μm) | 25, 50, or 100 | 25, 50, or 100 | 25, 50, or 100 | 130 | horizontally 4 pixels/mm | horizontally 4 pixels/mm |
| Number of Grey Scale Levels | 256 | 256 | 256 | 256 | 32 | 32 |
| Density Range (D) or screen brightness (L) | 0.15 to 2.5 | 0.1 to 3.0 | 0.1 to 2.5 | 0.15 to 1.8 | 50-0 ft. Lamberts | 50-0 ft. Lambert |
| Relationship of Grey Levels | Linear | Linear or Log. | Linear or Log. | Linear | Linear | Linear |

TABLE 2. IMAGE PROCESSING APPLICATION PROGRAMS.

Image Input:

KINGIN—loads an image from an IBM Drum Scanner tape into an image data set on disk.
 TECHIN—loads an image from a TECHOPS scanner tape into an image data set on disk.
 TAPEIN—loads an image from a standard tape into an image data set on disk.
 REFORMAT—reformats input data into selected processing format.
 GRAF—accepts line graphic input from Graf Pen.

Test Image Creation:

GRID—generates a test image on disk of a geometric grid.
 BAR—generates a test image on disk of a resolution bar chart.
 STAR—generates a test image on disk of a radial bar chart.
 LINWEDGE—generates a linear gray-scale step wedge (successive steps change by an equal increment).
 SQ2WEDGE—generates a non-linear gray-scale step wedge (successive steps change by $\sqrt{2}$).

Image Geometry Modification:

MAGNIFY—performs image magnification.
 REDUCE—performs image reduction.
 EXPAND—performs expansion of image by repeating pixel values.
 GEOM—performs image geometry modification by use of n'th order mapping function.

Image Enhancement:

DIRECT—computes directional derivative of an image.
 LAPLACE—computes Laplacian of an image.
 SPATIAL—applies a spatial filter algorithm to an image.
 ADJUST—converts intensity values of an image using a replacement table.
 COMBINE—combines two or more images into a composite image.

Information Extraction:

CLASSIFY—performs multispectral classification on registered multispectral images.
 ROSE—generates a rose diagram useful for geological fault analysis.

Image Computations & Statistics:

AREA—measures area within a specified intensity range included in a specified polygon.
 AREARECT—measures the area within a specified intensity range included in a specified rectangle.
 HISTOG—outputs a histogram of an image on terminal or printer.
 SHADE—outputs a shade print of an image on terminal or printer.
 COEFF—computes mapping function coefficients for GEOM command.
 ACCUR—computes accuracy of mapping function.

Image Output:

KINGOUT—outputs an image to tape in format compatible with IBM Film Plotter.
 TAPEOUT—outputs an image to tape in standard image processing format.

Image Display:

IMPOUT—directs image data to the on-line Imagery Printer
 GSGERASE—erases on-line Gray Scale Display screen.
 GSGOUT—directs image data to the on-line Gray Scale Display.
 GCTERASE—erases on-line graphic computer terminal screen.
 GCTOUT—directs image data to the on-line GCT display.

Utility Functions:

LOGON—initiates a terminal session allocating resources required for the session.
 LOGOUT—terminates a terminal session.
 SAVE—permanently saves a temporary image under a user specified name.
 TABLE—creates or updates a data table for input to the ADJUST, AREA, CLASSIFY, SHADE or ROSE commands.
 SELECT—selects an image area for further processing by creating a new disk image dataset.
 CATALOG—lists images and tables saved by users.
 WHOUSER—lists the IDs of the active users.
 REMOVE—removes a specified dataset from the system.
 CHANGE—changes the name of an existing dataset.
 RESERVE—allocates the initializes disk space for an image.
 SIZE—lists the size of an image dataset in terms of pixels and lines.
 CLEAR—frees all system files.
 TIME—displays CPU, execution, and session time used during terminal session.

pling of the input data to obtain output intensity values.

Geometric Errors. The principal geometric errors associated with the data received from the MSS are illustrated in Figure 3. Brief explanations of these errors are—

- **Earth Rotation**—As the MSS completes successive scans, the earth rotates beneath the sensor. Thus the ground swaths scanned by each mirror sweep gradually migrate westward. This effect causes along-scan distortion.
- **S/C Velocity**—If the spacecraft velocity departs from nominal, the ground track covered by a fixed number of successive mirror sweeps changes. This produces a cross-scan scale distortion.
- **Altitude**—Departures of the spacecraft altitude from nominal produce scale distortions in the sensor data. For the MSS, the distortion is along-scan only and varies with time.
- **Attitude**—Nominally the sensor axis system is maintained so that one axis is normal to the earth's surface and another is aligned with the spacecraft velocity vector. As the sensor departs from this attitude, geometric distortions result. For the MSS, the full attitude time history contributes to the distortion.
- **Perspective Projection**—For some applications it is desired that LANDSAT images represent the projection of points on the earth upon a plane tangent to the earth, with all projection lines normal to the plane. The sensor data represent perspective projections, i.e., projections whose lines all meet

at a point above the tangent plane. For the MSS, this produces only along-scan distortion.

- **Scan Skew**—During the time that the MSS mirror completes one active scan, the spacecraft moves along the ground track. Thus the ground swath scanned is not normal to the ground track but is slightly skewed. This produces cross-scan geometric distortion.
- **Panoramic Distortion**—Nominally, data samples are taken at regular intervals of time (and, hence, nominally at regular spatial intervals on the ground). In reality, the ground area imaged is proportional to the tangent of the scan angle rather than to the angle itself. This effect produces along-scan geometric distortion.
- **Mirror Velocity**—The scanning mirror of the MSS nominally moves at a constant angular rate. In reality, the mirror rate varies across a scan. Since data samples are taken at regular intervals of time, the varying mirror rate produces along-scan geometric distortion.
- **Map Projection**—For some applications, production of output products in a specific map projection is desired. Although map projection does not constitute an actual geometric error, it does require a geometric transformation of the input data and can be accomplished in the same operation that compensates for the distortions present in the data.

Determination of Error Magnitudes. If such errors are to be corrected, they must be either predictable or measurable. Errors due to MSS mirror velocity, panoramic distortion, scan skew, and perspective projection are systematic and stationary. That is, the effects are constant (for all practical purposes) and can be predicted in advance. Errors due to spacecraft velocity are a known function of that velocity, which can be obtained from tracking data. Errors due to earth rotation are a function of spacecraft latitude and orbit and thus also can be predicted from tracking data.

Attitude and altitude errors are neither systematic nor stationary. If they are to be corrected, their effects must be measured for each image. The measurement technique used here involves apparent displacements of ground control points (GCP's), detectable and recognizable geographic features whose geographic positions are known. The image locations of the GCP's are determined by application of a control location algorithm to appropriate areas of sensor data. For the MSS, differences between the actual and observed GCP locations are used to evaluate the coefficients of cubic time functions of roll, pitch and yaw, and a linear time function of altitude.

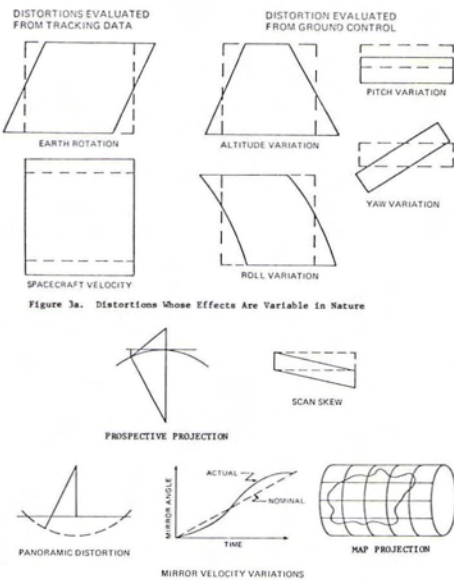


Figure 3a. Distortions Whose Effects Are Variable in Nature

Figure 3b. Distortions Whose Effects Are Systematic in Nature

FIG. 3. MSS geometric distortions.

Geometric Correction Function. The image spaces and transformations used in the geometric correction of MSS data are shown in Figure 4. The input image is an array of digital data which represents a geometrically distorted one-dimensional perspective projection of some portion of the earth's surface. The output image is a geometrically correct map projection of the same ground area.

GCP's are located in the input image and are mapped into the tangent plane by using models based on all those errors which can be predicted or determined from tracking data. The nominal GCP locations are mapped from the map space to the tangent plane through the equations that relate points in map or tangent plane space to points on the earth's surface. The nominal and observed GCP locations in the tangent plane are then used to evaluate the coefficients of the attitude and altitude models. The error models and the map projection equations together provide the correction functions needed to relate points in the output space to points in the input space.

Rather than apply the correction functions to all points of the output image, an interpolation grid is established on the output image. This grid is constructed so that, if the four corners points of any grid mesh are mapped with the correction functions, all points interior to the mesh can be located in the input image with sufficient accuracy by bilinear interpolation on the corner points. (See Figure 5.)

Resampling. If the input data values are considered to lie at points on a regular lattice, the situation shown in Figure 6 occurs. The input space has been sampled at the points represented by the data values. When an output image point is mapped into the image space, its location does not generally coincide with any of the input sample points. In order to establish a data value for the output point, the input space must be resampled at the output point location.

There are at present three different resampling techniques being advocated for LANDSAT data. The simplest of these is nearest-neighbor assignment, in which the value of the closest input sample (point 11 in the example shown in Figure 6) is assigned to

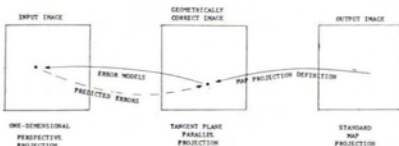


FIG. 4. MSS image spaces and transformations.

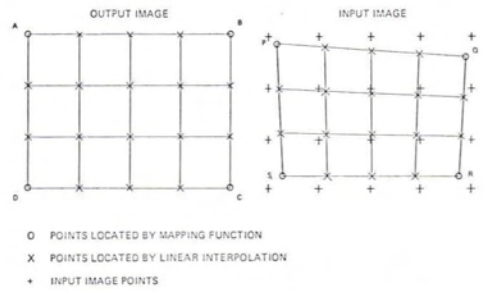
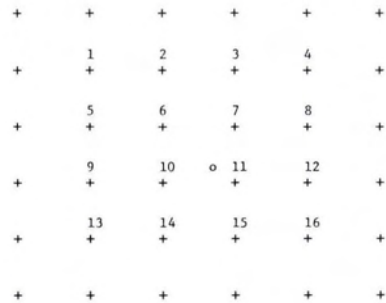


FIG. 5. User of linear interpolation in the mapping operation.

the output point. The second technique is two-dimensional linear (hence, bilinear) interpolation over the four surrounding input values (points 6, 7, 10, and 11 in Figure 6). Bilinear interpolation takes approximately ten times as long as nearest-neighbor assignment when implemented on a general-purpose computer. The third resampling technique is cubic convolution.⁹ Cubic convolution uses the sixteen input values closest to the output point in question and provides a higher order approximation to a sin x/x interpolator (theoretical resampling function). It runs approximately 20 times as long as nearest-neighbor assignment when implemented on a general-purpose computer. Figure 7 presents examples of LANDSAT MSS data resampled by IBM using these three techniques.

TYPICAL RESULTS

The IBM Image Processing Facility has



+ - INPUT IMAGE DATA VALUES
o - MAPPED OUTPUT IMAGE POINT

NEAREST NEIGHBOR ASSIGNMENT USES POINT 11
BILINEAR INTERPOLATION USES POINTS 6, 7, 10, AND 11
CUBIC CONVOLUTION USES POINTS 1 THROUGH 16

FIG. 6. Resampling geometry.

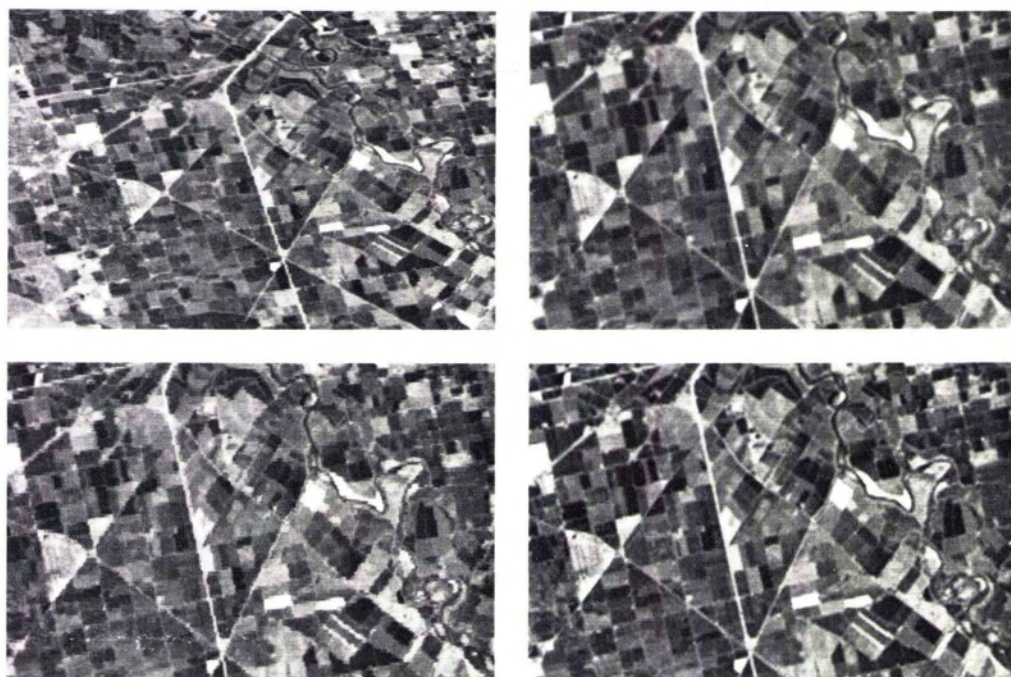


FIG. 7. Resampling results.

Upper left—original data.

Lower left—nearest-neighbor assignment.

Upper right—bilinear interpolation

Lower right—cubic convolution.

been used to support a variety of investigations. Two typical experiments, mosaicking and multispectral classification of mineral deposits, are discussed.

MOSAICKING

A growing number of applications require the combination or mosaicking of several LANDSAT scenes. Under contract to the Department of Interior Bureau of Land Management, IBM completed an experiment to demonstrate the feasibility of forming such mosaics digitally.⁷ Eight MSS scenes, whose relative geometry is shown in Figure 8, were chosen for the experiment. Since the four scenes from each pass were originally continuous strips of data, the first step in the processing was to reformat the data as two continuous strips, eliminating the along-track overlap.

Geodetic coordinates for 75 GCP's, whose approximate locations are shown in Figure 8, were measured by the BLM from 1:250,000 or 1:24,000 scale maps and provided to IBM. The image coordinates of these GCP's were determined by using computer-generated shade prints. For each strip, a computer pro-



FIG. 8. Mosaicked scenes.

gram was used to compute correction functions which transformed the GCP locations so that they were located in their proper positions in a UTM projection. For the pass 1372 strip, a second function also was computed. This function transformed the GCP's in the overlap region only to bring them into coincidence with those of the pass 1373 strip. The two correction functions for the pass 1372 strip were then combined in a single composite transformation. The two strips of data were then corrected geometrically by using the composite transformation. Registration of the two corrected strips was achieved by examination of shade prints.

The remaining problem concerned the elimination of the duplicate data in the overlap region. This was accomplished by a program which accepted as input a boundary specified as a sequence of straight line segments. Data to the left of the boundary were taken from the left-hand strip; data to the right of the boundary were taken from the right-hand strip. The mosaicked array was trimmed down to fit the capacity of IBM's drum film recorder, and a border including annotation and geodetic tick marks was added. The composite array was recorded on film at 1:1,000,000 scale using a 50 μ m square spot.

The processed mosaic is shown in Plate 1. Excellent geometric fitting has been accomplished and scene discontinuity results only from cloud patterns and radiance differences due to time separation between the data.

MULTISPECTRAL CLASSIFICATION OF MINERAL DEPOSITS

Under a contract with the U. S. Geological

Survey, a LANDSAT MSS scene of the western Chagai District, Pakistan was processed, and computer-aided information-extraction experiments were conducted to identify potential sulfide ore-bearing localities.⁸ The experimental approach is summarized in Figure 9. Shown there are the source data used, the digital processing applied to the source data, the products generated, the analysis conducted, and the final products. By a combination of digital image processing and information extraction, and manual analysis and evaluation, three processing operations were performed: digital image generation, support data generation and analysis, and multispectral classification.

Digital image generation. The uncorrected LANDSAT MSS data was reformatted into 185 km \times 185 km areas, and each band was radiometrically (intensity) adjusted and systematically geometrically corrected. The resulting computer-compatible tapes (CTT) were then recorded on film from which black-and-white and color prints were made. These prints were used as aids in the selection of the field prospecting sites during the evaluation of the classification results and also during the field checking. A color composite of the processed scene is reproduced on the cover.

Support data generation and analysis. The formatted but uncorrected CCT's were used for analysis prior to the multispectral classification operation. Shade prints (computer printouts providing the reflectance sensed in each spectral band) for selected areas were prepared and used as maps for precise location of individual data rectangles (pixels) relative to known ground features and known rock types. Numeric data for the 4 MSS bands

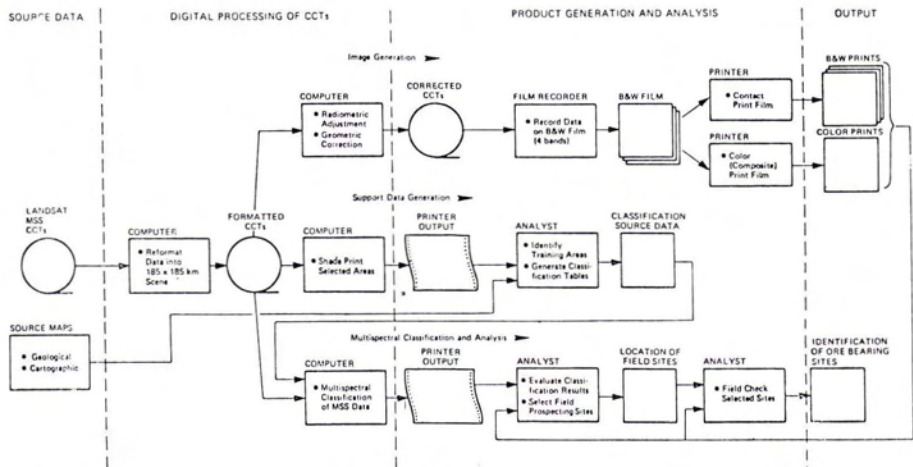


FIG. 9. Graphic summary of digital processing and data analysis performed in the experiment.

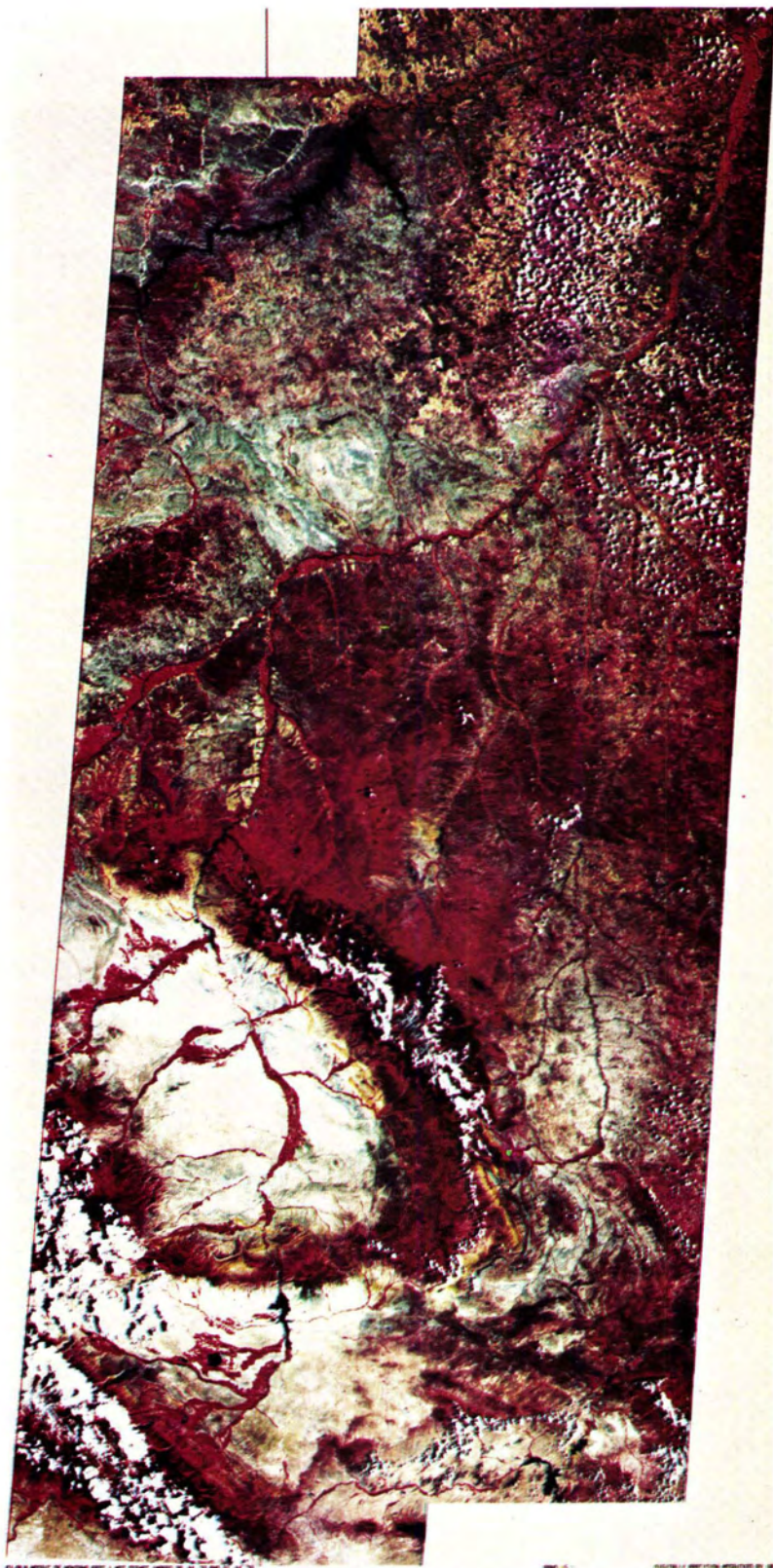
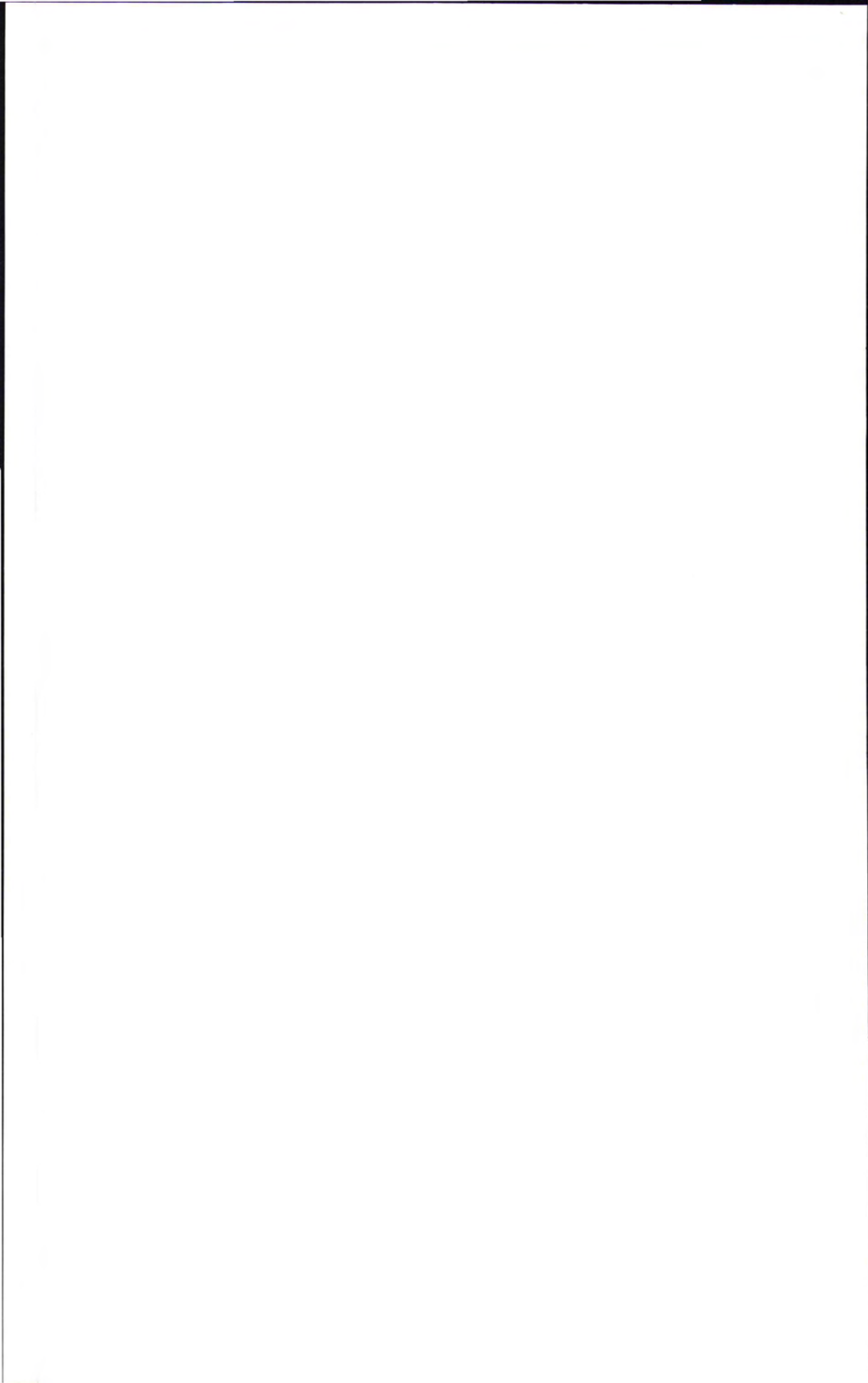


PLATE 1. Digitally mosaicked LANDSAT MSS scenes.



were extracted for each pixel in the known areas, and maximum and minimum sensed-reflectance limits were chosen for each rock type. A known copper sulfide-bearing deposit at Saindak was the source of data used to prepare the classification tables. Five revisions were made and tested, and one alternate classification table was tried. These tables were then used on an interactive basis to classify a nearby region within the same LANDSAT scene in which copper sulfide-bearing areas were suspected but in which no deposits were known (application area).

Multispectral classification and analysis. A spectral-intensity discrimination program was used for multispectral classification on the application area using the tables prepared for the Saindak deposit. The program tested the reflectance of each picture element within the application area against the maximum and minimum reflectance limits in the table and determined into which surface class (rock type) the picture element belonged. The symbol for that class was printed on a computer listing as part of a classification map. When the observed values fit more than one class (when classes were set up with overlapping limiting values), a pixel was placed in the class that was considered first in the search sequence.

The classification table resulting from five revisions was used to evaluate an adjacent area of 2100 km² considered to have good potential for porphyry copper deposits in the western Chagai Hills. The results were printed-out in 13 computer-generated vertical strip maps. These maps were examined for groups of pixels classified as mineralized quartz diorite and pyritic rock, and about 50 groups or concentrations were identified. Each was then evaluated for probability of correct classification, relationship to concentrations of other classes, and comparison with known rock types and occurrences of hydrothermal mineralization. From this examination, 30 localities most deserving reconnaissance checking in the field were chosen. The locations of these targets were marked on an enlarged (1:250,000) digitally enhanced image of MSS band 5 in order to simplify location on aerial photographs and in the field.

As part of the field check, all anomalous areas were first examined on stereoscopic pairs of 1:40,000-scale aerial photographs; at this point, it was possible to reject seven areas as related to windblown sand. Nineteen sites were examined in the field, and four desirable sites were not reached in the field checks. Five sites were found to be extensive out-

crops of hydrothermally altered sulfide-rich rock. Two additional sites contain altered rock with some sulfide but seem less attractive for prospecting at this time.

CONCLUSIONS

Digital image processing techniques and systems will play a progressively larger role in future imaging applications. This is due in part to the emerging digital sensors that have demonstrated their spatial and spectral utility on the LANDSAT program, the flexibility and performance that can be achieved with general and special purpose digital hardware, and the rapid advance of digital information extraction programs such as multispectral classification.

ACKNOWLEDGMENTS

A number of people have contributed to the technology and system discussed in this paper. These people include M. Cain, R. Cannizzaro, B. Clark, C. Colby, R. Depew, S. Murphrey, W. Niblack, N. Rossi, and S. Shapiro. The mineral deposit experiment was performed cooperatively with R. G. Schmidt of the U.S. Geological Survey, and his significant effort is acknowledged. The mosaicking experiment was sponsored by G. Torbert of the U. S. Department of Interior, Bureau of Land Management; his contribution and support are sincerely appreciated. The image correction work described in this paper was partially supported under NASA Contract NAS5-21716.

REFERENCES

1. Mercanti, E. "The ERTS-1 Experiments Teaching Us a New Way to See," *Astronautics and Aeronautics*, Sept. 1973, Vol. 11, No. 9.
2. *ERTS Data Users Handbook*, NASA—Goddard Space Flight Center, GE Document #71SD4249.
3. *Specifications for EOS System Definition Studies*, Earth Observatory Satellite (EOS) Project, Goddard Space Flight Center, Document No. EOS-410-02, September 13, 1973.
4. R. Bernstein, "Results of Precision Processing (Scene Correction) of ERTS-1 Images Using Digital Image Processing Techniques", *Symposium on Significant Results Obtained from the Earth Resources Technology Satellite-1*, Vol. II, NASA Document #SP-327, March 5-9, 1973.
5. R. Bernstein, "Scene Correction (Precision Processing) of ERTS Sensor Data Using Digital Image Processing Techniques", *Third ERTS Symposium*, Vol. 1, Section A, NASA SP-351, December 10-14, 1973.
6. R. Bernstein "All-Digital Precision Processing

of ERTS Images", Final Report, NASA Contract NAS5-21716, April 1975.

7. Bernstein, R., D. G. Ferneyhough and S. W. Murphrey, *Final Report—Feasibility of Generating Mosaics Directly from ERTS-1 Digital Data*, IBM Report No. FSC 74-0140, April 30, 1974.
8. Schmidt, R. G., B. B. Clark, and R. Bernstein, "A Search for Sulfide-Bearing Areas Using

LANDSAT-1 Data and Digital Image Processing Techniques," presented at the NASA Earth Resources Survey Symposium, Houston, Texas, June 1975.

9. Rifman, Samuel S., "Evaluation of Digital Correction Techniques for ERTS Images—Final Report," TRW Systems Group Report 20634-6003-TU-00, March 1974.

Report

35th PHOTOGRAMMETRIC WEEK STUTT GART, SEPTEMBER 8-13, 1975

The Photogrammetric Week, under the scientific supervision of Prof. Friedrich Ackerman/Stuttgart University and Dr. H. K. Meier/Carl Zeiss Oberkochen, West Germany, proved again its importance and attraction to the photogrammetrists of the world. Twenty high level invited papers were presented to more than 250 participants from 38 nations from all continents. The opening and welcome address was presented by the president of Stuttgart University, Prof. Hunken, and Prof. Dr. Kurt Schwidewsky, who presided over so many Photogrammetric Weeks in the past, also welcomed the audience and discussed in a humorous way the question of how he himself got into photogrammetry.

Three main subjects were chosen as the scientific basis of the 35th Photogrammetric Week:

- (1) The present status of the art of photogrammetry and remote sensing.
- (2) The technical procedure and status of aerial photography and data processing.
- (3) Computer supported stereoplotting.

The last subject, the main topic of this Photogrammetric Week, is related to nearly all branches of photogrammetric activity. This was also reflected in the selection of papers ranging from block triangulation to orthophoto technique and from remote sensing to pure analytical plotting. Optical and electronic image processing and a review of the electronic computing aids were described and discussed. Speakers from private and industrial companies told of their efforts

using computer controlled geodetic data banks, a system called GEOMAP, and how computer supported cartography is applied.

Speakers from Carl Zeiss Oberkochen reported in three papers about the new instruments recently developed at their laboratories. The DIRECT 1, the Stereocord G-2 and the DZ-5, a computer supported digital coordinatograph.

All papers were simultaneously translated into English, French, Spanish and Italian. Each paper was followed by a lively discussion, which sometimes revealed opposing viewpoints, but always increased the participation of the audience. Two afternoons were reserved for the demonstration of the photogrammetric instruments of the Institute of Photogrammetry of the University of Stuttgart. Much attention was paid to the new instruments developed by Carl Zeiss Oberkochen which were demonstrated, and each participant had an opportunity to work with them briefly. On Thursday, September 11th, an excursion was arranged to Oberkochen, site of the Carl Zeiss factory, where the production of optical mechanical and electronic equipment was demonstrated. Most impressive were the large and extremely precise mirrors with diameters up to 2.2 meters for astronomical telescopes. A delightful social get together, with dinner at the famous Wuerttemberg wine village of Struempfelbach concluded the day with lots of songs and "Vierteles."

—Herbert F. Trager